# Shape, firmness and fruit quality QTLs shared in two non-related strawberry populations

Pol Rey-Serra [a,b], Mourad Mnejja [a,b], Amparo Monfort [a,b,*]

[a] Centre for Research in Agricultural Genomics (CRAG), CSIC-IRTA-UAB-UB, Bellaterra, Barcelona, Spain
[b] Institut de Recerca i Tecnologia Agroalimentàries (IRTA), Barcelona, Spain

ARTICLE INFO

ABSTRACT

The cultivated strawberry (Fragaria x ananassa) is an octoploid species ($2n = 8x = 56$), appreciated widely for its fruit. There have been very few studies on fruit quality traits, which are known to be mostly polygenic and environmentally dependent. To identify higher genetic variability, two non-related populations were genotyped: an F1 population cross between 'FC50' and 'FD54' and an F2 population cross between 'Camarosa' and 'Dover', hybridizing both with IStraw35k and IStraw90k SNP arrays, respectively. The F1 genetic map was constructed with 14595 SNPs and the F2 map with 7977 SNPs. High collinearity was observed when comparing one genetic map with the other and on comparing both with the octoploid genome. To assess fruit variability, both populations were phenotyped for shape, firmness, taste and other fruit traits over the 2016−2019 period. With QTL analyses, 33 stable QTLs were mapped in the 'FC50xFD54' population, and three hotspot regions were found for shape traits in LG3A, LG4D and LG6D. In the '21AF' population, only eight stable QTLs were detected. Despite that, two major and stable QTLs were mapped in the same interval of confidence for both populations. A shared fruit shape ratio QTL which explained around 25 % of trait variance was mapped in LG3A, and a shared firmness QTL explaining 26.9 % of trait variance in LG7C. For the first time, two QTLs were discovered in LG3A and LG4A for a phenotype neck without achenes. When analysing two different mapping populations, in addition to finding specific QTL regions for the studied traits, a narrowing down of the interval of confidence for the shared QTLs is achieved. As a result of this study, a new set of SNPs for fruit firmness and shape is now available for use in MAS in strawberry breeding programs.

## 1. Introduction

The cultivated strawberry (Fragaria x ananassa), a member of the Rosaceae family, is the most highly appreciated berry in the world. Consumer acceptance lies in the balance between sweetness and acidity of fruit as well as perception of certain volatile compounds. Additionally, traits such as firmness and shape are very important for the commercial value of these fruits. Although breeding programs have traditionally focused on agronomical traits, improving fruit quality traits is becoming increasingly important.

F. x ananassa is an allo-octoploid species ($2n = 8x = 56$) with a highly diploidised behaviour. To determine the heritability of certain traits, constructing a genetic map for a segregating population is the first step for analysis of quantitative trait loci (QTL). The first strawberry genetic map was generated with transferable SSRs, using the Fragaria vesca diploid map [1] as a model, allowing the construction of low density octoploid maps [2–4]. With the emergence of high-throughput SNP markers, different SNP arrays have been developed for cultivated strawberry. The first was the IStraw90k based on the polymorphism detected between short-read sequences of three diploid species of Fragaria and 19 accessions of the three octoploid species aligned to F. vesca genome [5], then the improved IStraw35k SNP array derived from the previous IStraw90k SNP array [6]. The availability of these tools prompted the construction of new genetic maps, the principle objective being to discover loci implicated in resistance to certain airborne fungal diseases [7,8]. These dense genetic maps permit the narrowing down of QTL size in order to find markers with higher correlation to the trait. However, few of these genetic maps were designed for fruit quality QTLs. Recently, thanks to the sequencing of the cultivated strawberry genome [9], an 850k array and an improved 50k array with specific sub-genomic markers has emerged [10].

The ratio of sugars to acid content is important to the flavour of

strawberries. Sweetness perception in fresh fruits is highly correlated to the major sugar content being glucose, fructose and sucrose compounds. Soluble solids content (SSC) is an easy approach when quantifying sweetness. In cultivated strawberry, several QTLs for SSC have been mapped in different homeologous groups (HGs), HGII, HGIII, HGV and HGVI [2–4], showing polygenic heritability. Concerning the acidity traits, several regions responsible for acidity content, measured as titratable acidity (TA) and pH, have been mapped in HGI, HGIII, HGIV and HGV in different F1 populations [2–4]. The sugar-acid ratio (SAR) is used to quantify the balanced fruit taste and a SAR QTL has been mapped in LGVI3 [4]. Looking at the metabolite QTLs, fructose, glucose and sucrose QTLs have been detected in the majority of the homeologous groups in the octoploid population [3] and in a diploid NILs collection [11], as observed for citric and malic acid QTLs [3]. Furthermore, primary metabolite QTLs have been correlated with some fruit quality QTLs [12].

Strawberries are soft fruits characterized by a very short shelf-life, making fruit firmness an important trait from a commercial point of view. However, even though several cell-wall modifying enzymes involved in fruit firmness have been studied [13–17], little is known about its regulation.

The shape of the fruit is a hormone-regulated trait, in which auxins and GA modulate diameter and length, while ABA inhibits growth and induces the ripening of fruit in the final stages [18,19]. There are many factors that can alter the final fruit shape: two round fruit shape QTLs in LG2 and LG5 and a QTL for elongated fruit shape in LG5 [11] have been mapped in a diploid NILs population.

Despite these QTL analyses in different strawberry populations, only a low level of collinearity has so far been detected in the same fruit quality traits of different populations.

The aim of this study was to find stable QTLs and syntenic regions associated both with strawberry appearance and fruit quality traits, over a period of years, by constructing high-density genetic maps using the progeny of two bi-parental populations of crosses 'FC50' x 'FD54' and 'Camarosa' x 'Dover'.

## 2. Materials and methods

### 2.1. Plant material

Two advanced breeding lines (PLANASA), 'FD54' derived from the cross between cultivars 'Darselect Bright' and 'Candonga' and 'FC50' from the cross between 'Donna' and 'Cigaline', were crossed to obtain an F1 population (hereafter, 'FC50xFD54'), segregating for firmness, shape and perception of flavour. 'FC50' has a wild strawberry aroma, whereas 'FD54' has a characteristic fruity aroma. At least six clonal runner plants per progeny, parental and grandparental lines were grown using standard cultivation practices in the south-west of France (Le Barp, latitude: 44°67'N, longitude 0°73'W) for three successive years (2017−19). Fruits were collected in six harvests over three years at the stage considered by breeders as commercially mature, based on external colour. Harvests from the same year were then collected at one to two-week intervals between May and June. The plants were replicated clonally each year by runners. At the end of the assay, 63 seedlings were analysed from all harvests.

Two commercial cultivars, 'Dover' and 'Camarosa', were crossed to obtain a hybrid ('H-21') which produced an F2 population of 117 progeny lines (hereafter, '21AF'). Grown in a north-eastern region of Spain (Caldes de Montbui, latitude: 41°36'N, longitude 2°10'E), mature fruits of each progeny were collected three to five times per year over three years, between May and July.

All fruit phenotypic data were recorded immediately or at the most, three days after collection, maintaining the fruits in a cold room, at 4 °C. Data from the 'FC50xFD54' population were averaged independently for each of two harvests every year, whereas the data were averaged in the case of the '21AF' population on a single harvest per year.

### 2.2. Genetic map and genome comparison

DNA was extracted from young leaves following a modified method of [20] by adding 2% PVP to the CTAB solution. DNA concentration (30 ng/μl) and quality checked using a NanoDrop spectrophotometer and PicoGreen.

High quality DNA extractions from 56 genotypes from the 'FC50xFD54' population and both parental lines were hybridised with the Axiom® IStraw35 384 H T array (hereafter, IStraw35k array) [6], and the 117 genotypes from the '21AF' population and 'H-21', 'Camarosa' and 'Dover' parental lines with the IStraw90k SNP array [5]. Markers were clustered using the default parameters of the Axiom Suite software (Thermo Fisher Scientific, MA, USA).

Segregating markers with more than 17 % missing calls and distorted segregation ($\chi^2$ test: p-value < 0.05) were removed. To create genetic maps, the JoinMap®5 software [21] was used, adopting Maximum Likelihood (ML) and LOD score >2 to split different linkage groups (LG), and using the CP and F2 population types for the 'FC50xFD54' and the 'Camarosa' x 'Dover' maps. Genetic distances were estimated using the Kosambi mapping function [22]. Possible wrongly genotyped markers were checked by the *Nearest neighbour stress* function. The different LGs were identified and named according to Hardigan et al. [23] and oriented as the *F. vesca* genome [24].

The sequences of the IStraw35k markers were blasted using default parameters to the *F. x ananassa* cv. 'Camarosa' v1 genome [9] so as to identify the physical positions of markers. Those markers that were mapped in a unique position, were then selected to find correspondence between LGs and chromosomes. In many cases, markers located in different homeologous chromosomes of the *F. x ananassa* genome, mapped to the same LG as in our map. In those cases, the most abundant chromosome for each LG was accepted as corresponding. For the maximum number of marker positions in the *F. x ananassa* genome, those markers with two hits were only added if they mapped to the corresponding LG.

### 2.3. Phenotype analysis

#### 2.3.1. Weight, firmness, SSC and acidity

Based on changes in colour and firmness, mature fruits from seedlings, parental and grandparental lines from 'FC50xFD54' were collected in 2017 and 2018. The ripe fruits from '21AF' parental lines, hybrid and progeny were collected in 2016 and 2017.

Fruit weight (FW) was taken as an average of five to seven fruits (Ohaus Corp., Switzerland). Firmness (FIR) of three to four fruits was estimated with a penetrometer (Fruit Test™, Wagner Instruments) in gr force units. The juice of three to four strawberries was used to measure soluble solid content (SSC) with a digital hand refractometer (Atago Co. Ltd., Tokyo, Japan), expressed in brix degrees. Five ml of juice diluted with 45 mL deionised $H_2O$ were measured in a HI 84532 titratable acidity Mini Titrator (Hanna instruments, Rhode Island, USA) reporting pH and titratable acidity (TA). TA is calculated by the quantity of NaOH (0.5 M) needed to reach pH 8.1 and reporting citric acid content (g/-100 mL). Ratios between sweetness and acidity (SAR) were calculated as index, SAR = 10*SSC/TA.

#### 2.3.2. Shape

Mature fruits from 'FC50xFD54' and progenitors were collected in 2017, 2018 and 2019, and mature fruits from '21AF' and parents in 2016, 2017 and 2019. Three to five fruits per progeny and parental line were cut longitudinally and each half was scanned. All scanned fruits were analysed with Tomato Analyser v4.0 software [25,26]. The most significant measurements of fruit shape were selected from data collected by software, such as fruit perimeter (FP), fruit area (FA), maximum fruit length (FL) and maximum fruit diameter (FD) in cm units. Two separate ratios were calculated based on these measurements, fruit shape ratio (FSR = FL/FD) and widest width position (WWP
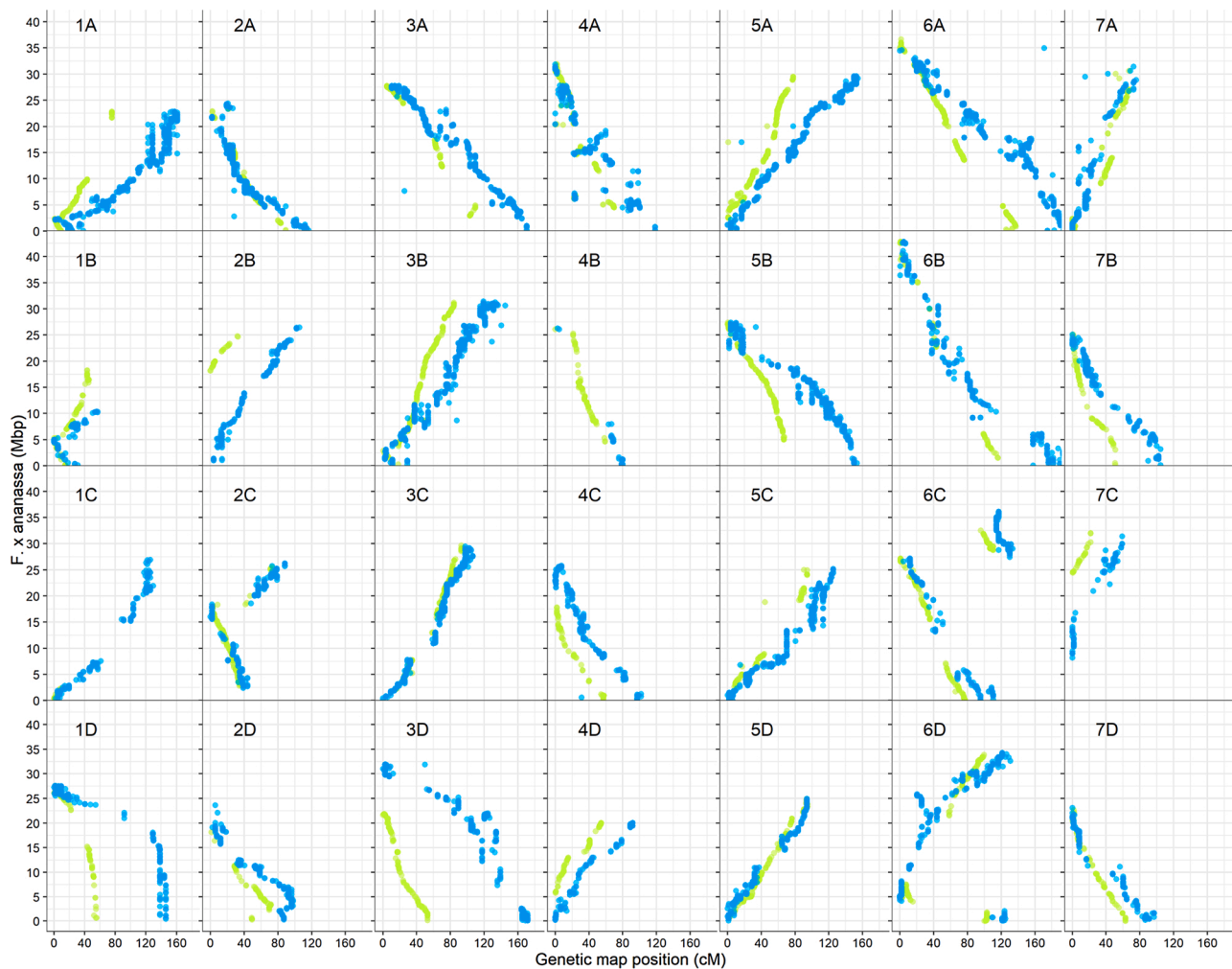
**Fig. 1. Collinearity of genetic maps versus octoploid genome**. Dot plot representing the relationship and collinearity between the genetic position of the markers in 'FC50xFD54' (blue) and '21AF' (green) genetic maps and physical position on the *F. x ananassa* genome, showing the correspondence between LGs and chromosomes (For interpretation of the references to colour in this figure legend, the reader is referred to the web version of this article.).

= y/FL), where 'y' is the height at which maximum width occurs. Error rates were calculated between measurements and the theoretical shapes such as elliptic (Ell) or circular (Cir) values, the further away from 0, the more dissimilar to that shape they become. Ovoid asymmetry (Ovo) and vertical asymmetry (VA) give high values when they have high asymmetry.

A neck phenotype was observed in 'FC50xFD54' progeny and described as a band without achene. A panel test characterised the scanned fruits from four harvests in 2017 and 2018 for presence or absence of neck. The proportion of fruits showing the neck phenotype in each progeny was used for QTL analysis.

### 2.4. Data analysis

The statistical analyses of the different traits were carried out using R v3.6.2 [27] with the Rstudio v1.2.5033 interface [28]. The Pearson correlation between harvests and traits were calculated using 'cor' function and visualised by the 'corrplot' R package (version 0.84). The Boxplots and *t*-test statistics were calculated using 'ggplot2' (version 3.3.0) and 'ggsignif' (version 0.6.0).

### 2.5. QTL analysis

Interval Mapping (IM) and the non-parametric Kruskal-Wallis (KW) test were used for quantitative trait analyses with the MapQTL®6

software [29]. The threshold to identify a major QTL was calculated by a permutation test and established at a LOD score of four. QTLs that mapped with a minimum LOD score of 2.5 by IM test in at least two harvests were considered as significant and stable, whereas QTL stability was considered in accordance with the number of significant harvests. The QTL size was determined as the overlapping 1-LOD confidence interval. Markers with the highest KW test in different harvests were considered the closest to each trait. The physical QTL mapping was visualized using the 'ggplot2' R package.

### 3. Results

#### 3.1. Genetic map

Two biparental populations were genotyped, with no pedigree relationship between the four parental lines as analysed by the Neighbour-joining method: the closest similarity was 60.38 % between the two progenitors 'FD54' and 'Camarosa'. The 'FC50xFD54' genetic map (F1 type population) was constructed with 14595 (52 %) markers from the IStraw35k SNP array, grouped in the expected 28 linkage groups (LGs) and spanning 3451.38 cM (Supplementary Table 1). This map had a high number of SNPs but only 2090 bins (groups of SNPs with the same genotype). Furthermore, in eight LGs (LG1C, LG1D, LG3C, LG3D, LG4B, LG5D, LG6B and LG7D) the gap was greater than 25 cM (Supplementary Fig. 1). SNPs with missing data and unlikely genotypes

**Table 1**

Summary of 'FC50xFD54' and '21AF' fruit quality traits. Mean and standard deviation (SD) of seventeen traits in parental lines 'FC50', 'FD54', 'Camarosa', 'Dover' and 'H-21' and mean, SD and range of the 'FC50xFD54' and '21AF' progeny.

| Traits | Abb. | FC50 | FD54 | FC50xFD54 | | Camarosa | Dover | H-21 | 21AF | |
|---|---|---|---|---|---|---|---|---|---|---|
| | | Mean ± SD | Mean ± SD | Mean ± SD | Range | Mean ± SD | Mean ± SD | Mean ± SD | Mean ± SD | Range |
| Fruit weight | FW | 15.69 ± 1.50 | **18.60 ± 1.50** | 15.95 ± 3.95 | 5.29 - 29.36 | 12.58 ± 1.15 | **18.42 ± 0.68** | 12.17 ± 2.17 | 10.80 ± 2.05 | 5.39 - 16.61 |
| Firmness | FIR | 298 ± 42 | 379 ± 87 | 356 ± 80 | 160 - 600 | 535 ± 67 | 467 ± 18 | 414 ± 19 | 451 ± 65 | 315 - 624 |
| pH | pH | 3.4 ± 0.2 | 3.5 ± 0.1 | 3.5 ± 0.2 | 3.1 - 4.0 | 3.6 ± 0.0 | 3.6 ± 0.0 | 3.4 ± 0.0 | 3.5 ± 0.1 | 3.3 - 3.7 |
| Titratable acidity | TA | 0.82 ± 0.13 | 0.77 ± 0.15 | 0.73 ± 0.14 | 0.31 - 1.11 | **0.94 ± 0.04** | 0.68 ± 0.06 | 1.03 ± 0.07 | 1.01 ± 0.15 | 0.59 - 1.52 |
| Soluble solids content | SSC | 9.6 ± 0.6 | 9.7 ± 0.8 | 8.9 ± 1.3 | 5.3 - 13.1 | 8.9 ± 0.9 | 7.3 ± 1.6 | 7.1 ± 0.5 | 8.2 ± 1.3 | 4.3 - 12.3 |
| Sweetness-acidity ratio | SAR | 119.08 ± 22.84 | 133.17 ± 42.17 | 126.24 ± 33.13 | 60.87 - 259 | 96.2 ± 15.42 | 110.16 ± 32.86 | 69.14 ± 9.67 | 82.99 ± 17.89 | 40.88 - 130.51 |
| Fruit perimeter | FP | 12.96 ± 0.76 | 13.45 ± 2.09 | 13.40 ± 1.55 | 8.38 - 20.40 | 12.29 ± 1.42 | 13.81 ± 0.61 | 12.27 ± 1.59 | 11.35 ± 1.13 | 6.25 - 14.35 |
| Fruit area | FA | 9.41 ± 1.38 | 9.78 ± 2.01 | 9.87 ± 1.70 | 4.40 - 16.78 | 8.85 ± 2.07 | 10.94 ± 1.16 | 8.71 ± 2.08 | 7.36 ± 1.37 | 2.60 - 11.44 |
| Fruit diameter | FD | 2.97 ± 0.25 | 3.23 ± 0.33 | 3.10 ± 0.30 | 2.03 - 4.06 | 3.21 ± 0.14 | **3.93 ± 0.56** | 3.26 ± 0.28 | 2.88 ± 0.27 | 1.84 - 3.66 |
| Fruit length | FL | 4.45 ± 0.38 | 4.29 ± 0.55 | 4.48 ± 0.52 | 2.96 - 6.14 | 3.76 ± 0.67 | 4.38 ± 0.25 | 3.86 ± 0.70 | 3.50 ± 0.44 | 2.24 - 4.90 |
| Fruit shape ratio | FSR | **1.51 ± 0.10** | 1.33 ± 0.05 | 1.45 ± 0.17 | 1.00 - 2.01 | 1.17 ± 0.16 | 1.28 ± 0.03 | 1.22 ± 0.12 | 1.23 ± 0.14 | 0.83 - 1.72 |
| Width-widest position | WWP | 0.36 ± 0.04 | **0.40 ± 0.02** | 0.37 ± 0.04 | 0.28 - 0.51 | 0.40 ± 0.05 | 0.35 ± 0.04 | 0.35 ± 0.03 | 0.36 ± 0.04 | 0.23 - 0.51 |
| Ellipsoid | Ell | 0.06 ± 0.01 | 0.06 ± 0.01 | 0.06 ± 0.01 | 0.03 - 0.12 | 0.06 ± 0.01 | 0.07 ± 0.01 | 0.07 ± 0.01 | 0.07 ± 0.01 | 0.03 - 0.10 |
| Circular | Cir | **0.15 ± 0.03** | 0.11 ± 0.01 | 0.14 ± 0.03 | 0.05 - 0.26 | 0.09 ± 0.03 | 0.11 ± 0.01 | 0.11 ± 0.02 | 0.10 ± 0.02 | 0.05 - 0.19 |
| Ovoid | Ovo | **0.28 ± 0.06** | 0.22 ± 0.02 | 0.26 ± 0.06 | 0.00 ± 0.13 | 0.24 ± 0.07 | 0.30 ± 0.05 | 0.29 ± 0.05 | 0.28 ± 0.06 | 0.06 - 0.49 |
| Vertical asymmetry | VA | 0.04 ± 0.01 | **0.05 ± 0.01** | 0.05 ± 0.02 | 0.02 ± 0.13 | 0.07 ± 0.01 | 0.09 ± 0.03 | 0.08 ± 0.01 | 0.07 ± 0.02 | 0.02 - 0.13 |
| Neck | Neck | 33.54 ± 29.00 | **77.50 ± 18.00** | 55.74 ± 36.44 | 0.00 ± 1.00 | – | – | – | – | – |

Bold and underlined numbers indicate the highest significant (p < 0.05) value in parental lines.

increase the genetic distances, so these markers were discarded, and with the remaining SNPs we built a more accurate and compact map with only one marker per bin (1461 bins). This map spans a total size of 2332.50 cM, with only three LGs (LG3A, LG6A and LG6B) over 120 cM, and was selected for QTL analyses.

The 117 seedlings from the '21AF' population (F2 type population) were hybridized with the IStraw90k SNP array. The genetic map was constructed with 7977 markers that were grouped in 28 LGs (Supplementary Table 1 and Supplementary Fig. 1) with 1990 bins covering a total genetic distance of 2056.42 cM. As with the 'FC50xFD54' genetic map, the '21AF' genetic map, only the best SNPs were retained and the map was reduced to 1457 bins and spanned a genetic distance of 1808 cM. The LG6C was split into two subgroups by discarding markers with missing data.

In addition, the marker position in both genetic maps was compared to the physical position in the *F. x ananassa* genome to verify its correct position and order (Fig. 1). When blasting the marker sequences to the *F. x ananassa* genome, 4060 markers were detected with a unique homology, enabling the identification of correspondence between LGs and chromosomes. Although the sequence of some markers was blast in multiple positions in homeologous groups, markers were localized in the correct LG thanks to information from both genetic maps. Furthermore, the 'FC50xFD54' genetic map covered 94.5 % of the genome, with the LGs covering more than 89.7 % of the corresponding chromosome length, except for LG1B which covered only 35 %, and LG7C which covered just 72 % of their corresponding chromosomes. Regarding the '21AF' genetic map, 12 LGs covered at least 90 % of the chromosome length, but others had reduced coverage, some less than 20 %, such as LG1C, LG2B and LG7C (Supplementary Table 1). High collinearity was observed between markers in both genetic maps, and also with physical positions in all LGs (Fig. 1), thereby confirming the quality of both

genetic maps. Only three LGs (LG2C, LG6C and LG6D) showed non-collinear regions with the physical positions. The observed negative collinearities in different LGs were due to map orientation with respect to the *F. vesca* genome (Fig. 1).

### 3.2. Fruit quality traits distribution and correlation in each population

The phenotypic data of the 'FC50xFD54' and '21AF' mapping populations from different harvests showed that the populations differ in major quality traits related to size, shape, firmness and taste of the fruit (Table 1 and Supplementary Table 2), where wider ranges were detected in 'FC50xFD54' for weight, firmness, sweetness and shape parameters. An example of the difference of fruit shape in both populations is shown in Fig. 2, a–b.

The distribution analysis of seventeen traits showed continuous variation in the seedlings of both populations, with a normal distribution for all traits, except for pH. The value range in both mapping populations was higher than in their parental lines. Additionally, there was a greater value range for the studied traits in the 'FC50xFD54' population than in the '21AF' population. Specifically, the 'FD54' parental line had higher values for fruit weight, firmness and taste traits compared to the parental line 'FC50', while the latter had higher values for shape traits related to fruit length. In the F2 population, in 'Camarosa' the values for fruit quality traits such as soluble solids content and titratable acidity were higher, but lower for fruit weight and other shape traits compared to 'Dover' (Table 1).

The relationship between traits of both populations was explored across different harvests using a Pearson correlation. In the 'FC50xFD54' population, stability was high across the harvests in all traits, except for SSC (Fig. 2c). Focusing on correlation between different harvests for each trait, correlation was higher in the 'FC50xFD54' population in
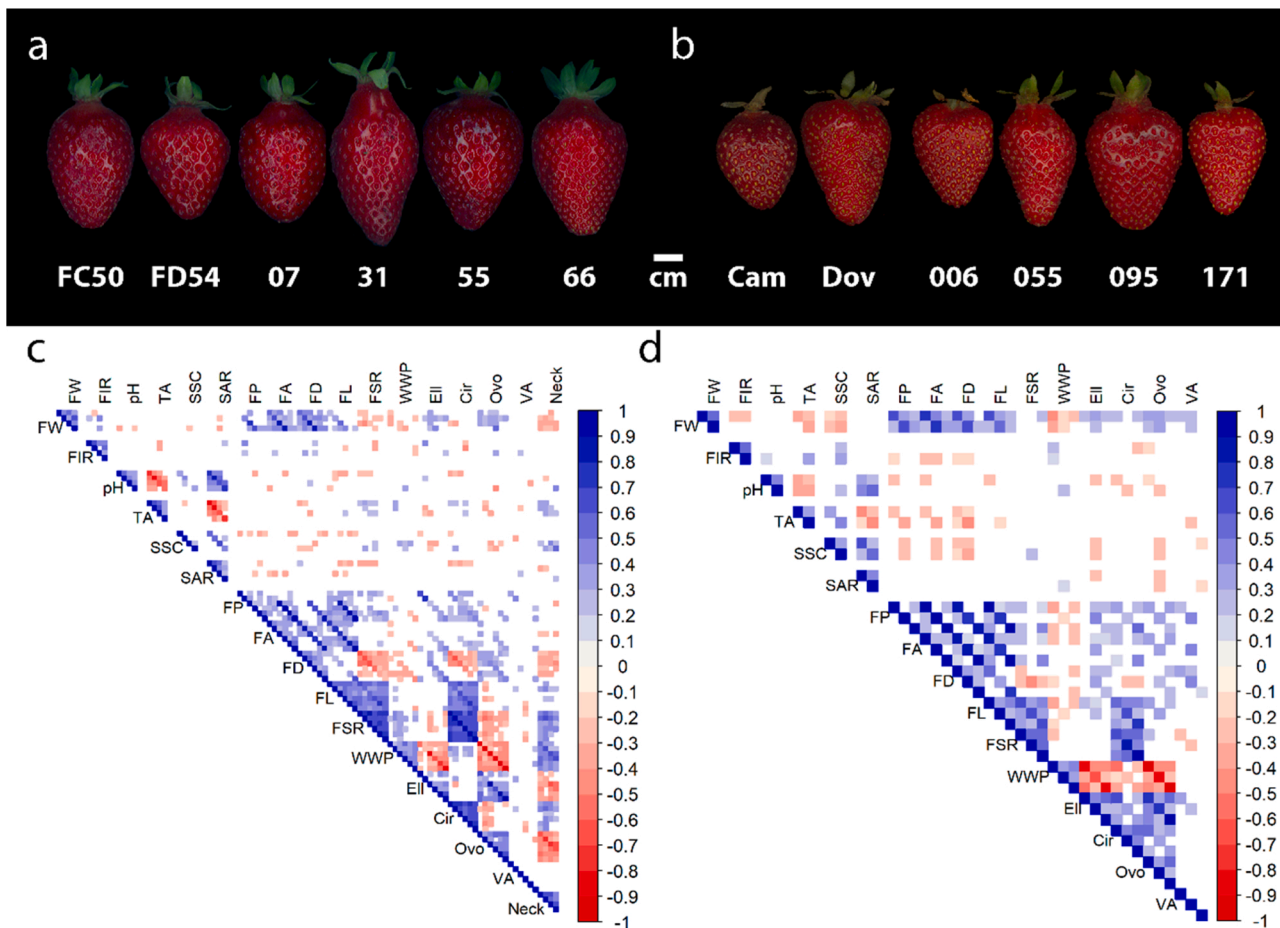
**Fig. 2. Variability and correlation of the traits in both populations.** Fruit shape observed in parental lines and siblings. a) 'FC50xFD54' and b) '21AF' populations. Heatmap visualization of Pearson correlation between fruit quality traits in different harvests. c). 'FC50xFD54' population data of six harvests (2017-19) and d) '21AF' population data in the three harvests (2016, 2017 and 2019). Blue-red colour range indicate positive-negative correlations, p-value<0.05 (For interpretation of the references to colour in this figure legend, the reader is referred to the web version of this article.).

almost all traits when compared with '21AF', with the exception of the FA, FD and FL shape traits (Fig. 2d).

Looking at taste traits, high correlations between acidity traits (pH and TA) and SAR were detected. Firmness is important for the commercial value of the strawberry, but it did not correlate with any other trait studied. In fruit shape analysis, the FW trait was highly correlated with direct shape measurements FP, FA, FD and FL, which were also highly correlated with each other. The positive correlation of fruit shape ratio (FSR) was higher for fruit length than that of the fruit diameter trait. The WWP ratio was negatively correlated with Ovo. Since the Cir error value showed a high correlation with FL and FSR, the longest fruits in these two populations were also the least circular. These correlations were found to be higher in the 'FC50xFD54' population than in the '21AF' population (Fig. 2, c–d).

Since the 'FC50xFD54' population had a neck phenotype segregation, a panel test was adopted for visual phenotype analysis. The correlations between harvests ranged from 0.45 to 0.67 and were even higher among panellists (0.53 – 0.82). Also, for neck trait, the correlations with the FSR and WWP ratios were highly positive whereas they were negative for Ovo, Ell, FW and FD measurements (Fig. 2c).

### 3.3. QTL analysis

QTL analysis was performed in both mapping populations to identify the genomic regions responsible for the phenotypic variability of the fruit quality traits. Since fruit harvests from different years are assumed to have different environmental characteristics, each harvest was analysed independently to assess QTL stability.

By phenotyping the 'FC50xFD54' population from six different harvests, 33 stable QTLs (LOD score > 2.5 in at least two harvest) were mapped. Ten were discovered in up to three or four of the six harvests, indicating stability throughout the harvests, with six of these considered major QTL with a LOD score above four. Of the stable QTLs, nine corresponded to weight, firmness and taste, with only one being major QTL (*SAR_1A*). Of the 24 QTLs detected for shape, five were considered major QTLs. A summary of the significant and stable QTLs in more than two harvests is given in Table 2 and visualized in Fig. 3 on the genome representation. The detail of the QTL data of all the crops is given in Supplementary table 3.

In the '21AF' population, 22 QTLs were mapped (Supplementary table 4), of which eight were registered in two harvests and one in all of three harvests (Table 2 and Fig. 3). Most of the stable QTLs were considered major, with LOD scores greater than four. In general, the highest incidence of variance observed in the '21AF' population (12−19 %) were lower than those detected in the 'FC50xFD54' population (22–37 %).

In relation to fruit weight, only two stable QTLs were detected in the 'FC50xFD54' population, both located at the beginning of the LGs, such as *FW_1A*, which explained between 21.3 and 27.8 % of the variance in all harvests, and *FW_3A* between 10 and 23.8 % of the variance.

Two QTLs for firmness were detected, in LG1A and LG7C. The *FIR_7C*, was the most important and mapped in both populations. In 'FC50xFD54', the *FIR_7C* was detected in three of the six harvests and explained a range of variance between 17.8 % and 26.9 %, and in '21AF'
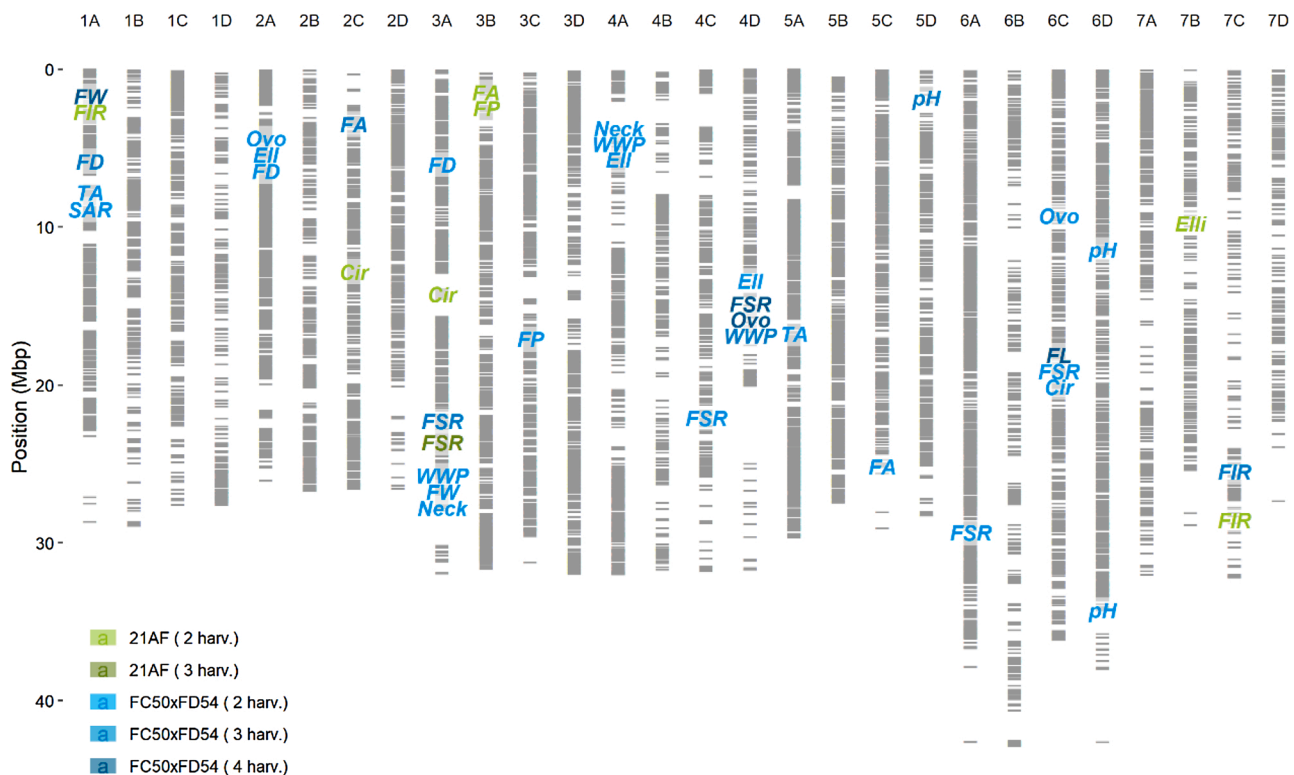
**Fig. 3. Map of fruit quality QTLs detected.** 'FC50xFD54' (blue) and '21AF' (green) QTLs mapped in the *F. x ananassa* genome. Colour intensity indicates stability. For trait abbreviation see Table 1 (For interpretation of the references to colour in this figure legend, the reader is referred to the web version of this article.).

it was major and stable in two of the three harvests and explained 14.5–17.8% of the observed variance (Table 2). The overlapping region in both populations covers 1.57 Mb of the genome, in a region containing 286 annotated genes. High synteny was found for both genetic maps in the region of the *FIR_7C* QTL (Fig. 4a). With the alleles from the most significant marker (Affx-88900969) in the *FIR_7C* QTL determined by the Kruskal-Wallis test, the 'b' allele in homozygosity was found to be statistically significant and linked to greater firmness, whereas the presence of the 'a' allele resulted in softer fruits in all harvests in both populations (Fig. 4a).

For the taste QTLs in the strawberry 'FC50xFD54' population, a total of six QTLs related to acidity were mapped. TA and SAR QTLs were located in the middle of LG1A, with *SAR_1A*, a major QTL explaining a maximum of 34.4 % of the phenotypic variance. The *SAR_1A* reduced the physical size of *TA_1A* to 1.87Mb and 276 annotated genes. Of the three QTLs detected for pH values, *pH_5D* was the most stable, explaining 13.6–25.8% of the acidity variance (Table 2). Despite the variability in SSC, no stable QTL was detected in order to explain this. In the '21AF' population, no stable QTLs for taste traits were detected, but several acidity QTLs, *pH_6A*, *TA_6A* and *SAR_6A*, were registered in one harvest while overlapping in the same region also (Fig. 3). In addition, four taste QTLs were located in homeologous groups and identified in one harvest only, such as *TA_3B* and *TA_3C* and *SAR_6A* and *SAR_6D2*, as observed for the firmness trait with *FIR_7B* and *FIR_7C* (detected in two harvests) (Supplementary table 4).

The analysis of fruit shape is more complex and for this reason, multiple traits were selected to better explain the real phenotypic variance. Three QTLs were mapped for the diameter of the fruit in LG1A, LG2A and LG3A (Table 2). The *FD_2A* mapped to the same position as *Ovo_2A* and *Ell_2A* (Fig. 3), which are related to the horizontal axis. The smallest QTL was *Ell_2A*, of 3.5 Mb and included 608 annotated genes. Only one QTL for fruit length was mapped in 'FC50xFD54', at the end of LG6C, being stable in four of the six harvests and contributing 14.1–24.5 % of the observed variance of the vertical axis. The *FL_6C* mapped to the

same position as the *FSR_6C* and *Cir_6C* and close to the *Ovo_6C* (Fig. 3). However, this QTL was large, 9.5 Mb, and included 1657 annotated genes. Three QTLs were detected for fruit area, two in 'FC50xFD54' (*FA_2C* and *FA_5C*), and one in '21AF' (*FA_3B*). The *FA_2C* QTL was the only major and stable QTL in three of the six harvests. One QTL for fruit perimeter was identified in the HG3 for each of the two populations, *FP_3C* in 'FC50xFD54' and a major *FP_3B* QTL in '21AF'.

Focussing on the ratio of the fruit shape, six QTLs were distinguished. *FSR_3A* was shared in both populations, being stable in three of the six harvests and explaining 10.9–24.8 % of the fruit shape ratio variance in 'FC50xFD54', and 11.1–16.2 % of the observed variance in '21AF' where it was detected in all harvests. There was high synteny for the *FSR_3A* region between both genetic maps (Fig. 4b) and the Affx-88834650 marker, located within the interval of confidence, had significant differences related to the fruit shape ratio between different genotypes, with the same behaviour in both populations. The 'a' allele in homozygosity was responsible for the fruit shape ratio increment in longer and narrower fruits (Fig. 4b). Closer to the shared *FSR_3A* QTL, two major QTLs related to fruit shape were also mapped, *Neck_3A* and *WWP_3A* (Fig. 3).

In addition to the shared *FSR_3A* QTL, other QTLs for the fruit shape ratio were found to map in the HG4 for the 'FC50xFD54' population, such as the major *FSR_4C* QTL, which generated a maximum of 29.3 % of the phenotypic variance, and a stable *FSR_4D* QTL detected in four of the six harvests, which explained 11.9–26.9% of the phenotypic variance. Three other QTLs related to the fruit shape trait were mapped in the same genetic region as *FSR_4D* (Fig. 3). The *WWP_4D* QTL, detected in three of the six harvests, explained 10.9–28.3% of the phenotypic variance. The major *Ovo_4D* QTL, which explained 11.6–36.8% of the observed variance, was recurrent in four of the six harvests. Finally, the major *Ell_4D* QTL produced a maximum of 31.2 % of the phenotypic variance. The overlapping region of the four previous QTLs was 1.5 Mb and enclosed 194 annotated genes. As in HG4, two other fruit shape QTLs were mapped in HG6, *FSR_6A* and *FSR_6C* (Table 2).

**Table 2**

**List of stable and significant fruit quality QTLs in both populations**, showing the number of harvests detected, the maximum values of LOD, % of variance explanation and KW test. Genetic map of each QTL as LG, QTL interval with initial and end position of the QTL and total size (cM) and physical location with chromosome, QTL interval (bp) and number of genes. Bold and underlined numbers in LOD, % Expl. and KW test indicate major QTLs.

| Population | QTL ID | Harv. | LOD | % Expl. | KW | Genetic map | | | Fxa genome | | | |
|---|---|---|---|---|---|---|---|---|---|---|---|---|
| | | | | | | LG | QTL interval (cM) | | Size (cM) | Chr. | QTL interval (bp) | | Genes |
| 'FC50xFD54' | FW_1A | 4 | 3.82 | 27.8 | 5.83 | 1A | 0.00 | 22.31 | 22.31 | Fvb1-4 | 305369 | 3402648 | 619 |
| 'FC50xFD54' | FW_3A | 2 | 3.12 | 23.8 | 11.31 | 3A | 0.91 | 11.98 | 11.07 | Fvb3-4 | 25009316 | 27774997 | 484 |
| 'FC50xFD54' | FIR_7C | 3 | 3.68 | 26.9 | 5.51 | 7C | 36.82 | 47.24 | 10.42 | Fvb7-1 | 22244345 | 28740635 | 1103 |
| 'FC50xFD54' | pH_5D | 3 | 3.44 | 25.8 | 13.45 | 5D | 0.00 | 2.73 | 2.73 | Fvb5-2 | 116223 | 3509049 | 585 |
| 'FC50xFD54' | pH_6D.1 | 2 | 3.46 | 25.5 | 15.82 | 6D | 14.90 | 18.30 | 3.40 | Fvb6-4 | 11412666 | 15043404 | 433 |
| 'FC50xFD54' | pH_6D.2 | 2 | 3.98 | 29.2 | 15.06 | 6D | 91.81 | 93.63 | 1.82 | Fvb6-4 | 30488840 | 34249264 | 622 |
| 'FC50xFD54' | TA_1A | 2 | 3.83 | 27.8 | 3.97 | 1A | 36.92 | 55.67 | 18.75 | Fvb1-4 | 5780396 | 9864602 | 669 |
| 'FC50xFD54' | TA_5A | 2 | 3.87 | 28.1 | 7.83 | 5A | 52.62 | 57.79 | 5.17 | Fvb5-1 | 13455988 | 20026637 | 831 |
| 'FC50xFD54' | SAR_1A | 2 | **4.77** | **34.4** | **17.60** | 1A | 39.92 | 49.17 | 9.24 | Fvb1-4 | 7430815 | 9308131 | 276 |
| 'FC50xFD54' | FA_2C | 3 | **4.20** | **30.1** | **15.67** | 2C | 0.00 | 29.87 | 29.87 | Fvb2-1 | 3493144 | 18383191 | 1821 |
| 'FC50xFD54' | FA_5C | 2 | 3.04 | 22.8 | 12.65 | 5C | 57.15 | 72.24 | 15.09 | Fvb5-4 | 13639694 | 25171401 | 1235 |
| 'FC50xFD54' | FP_3C | 2 | 3.28 | 24.0 | 14.13 | 3C | 49.33 | 63.65 | 14.32 | Fvb3-3 | 14538899 | 19667539 | 487 |
| 'FC50xFD54' | FL_6C | 4 | 3.29 | 24.5 | 10.16 | 6C | 52.85 | 68.53 | 15.68 | Fvb6-2 | 22393622 | 31885893 | 1657 |
| 'FC50xFD54' | FD_1A | 3 | 2.97 | 22.4 | 7.14 | 1A | 36.92 | 52.84 | 15.91 | Fvb1-4 | 5780396 | 9864602 | 669 |
| 'FC50xFD54' | FD_2A | 2 | 3.30 | 24.2 | 9.30 | 2A | 21.21 | 57.33 | 36.11 | Fvb2-2 | 3334456 | 9596766 | 1048 |
| 'FC50xFD54' | FD_3A | 2 | 3.05 | 22.9 | 12.21 | 3A | 95.93 | 106.06 | 10.13 | Fvb3-4 | 4403315 | 7654915 | 454 |
| 'FC50xFD54' | FSR_3A | 3 | 3.34 | 24.8 | 14.8 | 3A | 31.75 | 62.32 | 30.57 | Fvb3-4 | 16421818 | 24384706 | 1047 |
| 'FC50xFD54' | FSR_4C | 2 | **4.15** | **29.3** | **14.66** | 4C | 8.57 | 21.42 | 12.85 | Fvb4-2 | 16035844 | 22092362 | 513 |
| 'FC50xFD54' | FSR_4D | 4 | 3.68 | 26.9 | 11.81 | 4D | 54.51 | 62.01 | 7.50 | Fvb4-1 | 15125510 | 16588955 | 194 |
| 'FC50xFD54' | FSR_6A | 2 | 2.96 | 22.0 | 9.93 | 6A | 0.00 | 8.23 | 8.23 | Fvb6-1 | 26330087 | 32354801 | 1044 |
| 'FC50xFD54' | FSR_6C | 2 | 3.42 | 26.1 | 13.6 | 6C | 49.22 | 64.83 | 15.61 | Fvb6-2 | 22393622 | 31885893 | 1657 |
| 'FC50xFD54' | WWP_3A | 2 | **4.10** | **29.1** | **14.53** | 3A | 4.88 | 18.36 | 13.48 | Fvb3-4 | 25009316 | 27774997 | 484 |
| 'FC50xFD54' | WWP_4A | 2 | 3.73 | 26.8 | 11.48 | 4A | 56.49 | 61.90 | 5.41 | Fvb4-3 | 4032763 | 11434813 | 1233 |
| 'FC50xFD54' | WWP_4D | 3 | 3.76 | 28.3 | 9.31 | 4D | 54.51 | 62.01 | 7.50 | Fvb4-1 | 15125510 | 16588955 | 194 |
| 'FC50xFD54' | Ell_2A | 2 | 3.29 | 25.3 | 10.48 | 2A | 25.77 | 48.27 | 22.5 | Fvb2-2 | 4622446 | 8204317 | 608 |
| 'FC50xFD54' | Ell_4A | 2 | 3.01 | 22.7 | 13.67 | 4A | 56.49 | 63.77 | 7.28 | Fvb4-3 | 4032763 | 11434813 | 1233 |
| 'FC50xFD54' | Ell_4D | 2 | **4.22** | **31.2** | **8.80** | 4D | 55.51 | 61.20 | 5.68 | Fvb4-1 | 15125510 | 15677103 | 70 |
| 'FC50xFD54' | Cir_6C | 2 | 3.16 | 24.4 | 13.39 | 6C | 49.22 | 63.83 | 14.61 | Fvb6-2 | 22393622 | 31885893 | 1657 |
| 'FC50xFD54' | Ovo_2A | 2 | 3.08 | 22.7 | 11.16 | 2A | 24.77 | 51.33 | 26.56 | Fvb2-2 | 3334456 | 9410076 | 1018 |
| 'FC50xFD54' | Ovo_4D | 4 | **5.19** | **36.8** | **10.10** | 4D | 54.51 | 63.01 | 8.50 | Fvb4-1 | 15125510 | 16588955 | 194 |
| 'FC50xFD54' | Ovo_6C | 2 | 3.77 | 27.1 | 4.92 | 6C | 26.92 | 54.66 | 27.74 | Fvb6-2 | 144416 | 2513249 | 301 |
| 'FC50xFD54' | Neck_3A | 3 | **5.24** | **35.5** | **14.5** | 3A | 0.00 | 19.16 | 19.16 | Fvb3-4 | 25009316 | 27774997 | 484 |
| 'FC50xFD54' | Neck_4A | 2 | 3.94 | 28.1 | 14.96 | 4A | 57.48 | 73.96 | 16.48 | Fvb4-3 | 103787 | 11434813 | 1980 |
| '21AF' | FIR_1A | 2 | 3.48 | 13.1 | 15.07 | 1A | 0.00 | 23.25 | 23.25 | Fvb1-4 | 33866 | 4397357 | 872 |
| '21AF' | FIR_7C | 2 | **4.87** | **17.8** | **20.55** | 7C | 7.37 | 18.80 | 11.43 | Fvb7-1 | 27165768 | 29929846 | 506 |
| '21AF' | FA_3B | 2 | 3.55 | 13.9 | 15.18 | 3B | 4.80 | 13.44 | 8.64 | Fvb3-2 | 1256322 | 1671524 | 69 |
| '21AF' | FP_3B | 2 | **4.21** | **16.3** | **18.48** | 3B | 4.37 | 12.44 | 8.07 | Fvb3-2 | 1256322 | 1819447 | 88 |
| '21AF' | FSR_3A | 3 | **4.37** | **16.2** | **20.25** | 3A | 19.74 | 40.35 | 20.62 | Fvb3-4 | 24410717 | 24883703 | 85 |
| '21AF' | Ell_7B | 2 | 3.87 | 15.1 | 17.24 | 7B | 13.43 | 28.15 | 14.72 | Fvb7-3 | 8210045 | 11272705 | 429 |
| '21AF' | Cir_2C | 2 | 3.34 | 12.6 | 11.27 | 2C | 4.85 | 13.54 | 8.69 | Fvb2-1 | 12817036 | 16002613 | 432 |
| '21AF' | Cir_3A | 2 | **5.19** | **18.9** | **16.71** | 3A | 60.17 | 88.17 | 28.00 | Fvb3-4 | 12288855 | 16197763 | 473 |

Two QTLs mapped for the neck phenotype observed in the 'FC50xFD54' population and assessed by a panel test. The major *Neck_3A* QTL was detected in three of the six harvests, controlled a maximum of 35.5 % of the trait variance and colocalized with the major *WWP_3A* and the *FW_3A* QTLs. The presence of neck increased WWP ratios and decreased fruit weight. The other neck QTL, *Neck_4A,* also overlapped with *WWP_4A*, reducing the size of the QTL interval to a genetic distance of 11 cM and a physical distance of 4Mb.

For those genetic regions shared by fruit shape traits, two QTLs were identified in LG2C: *FA_2C* which explained between 13.0 and 34.1 % of the area variance of the 'FC50xFD54' population and *Cir_2C* for '21AF'. Furthermore, two '21AF' QTLs, both as detected in two of three harvests, were mapped at the beginning of LG3B for the correlated traits of area and perimeter, *FA_3B* and *FP_3B*, the latter being a major QTL that generated a maximum of 16.3 % of the phenotypic variance. The overlapping QTLs covered a region of 0.4 Mb including 69 annotated genes (Table 2).

The two populations were cultivated in different environments and some QTLs were detected in different HGs in each population, such as for the acidity trait *pH_6D* QTL for 'FC50xFD54' and *pH_6A* QTL for '21AF', or the fruit perimeter QTLs mapped in LG3C (*FP*_3C) for 'FC50xFD54' and in LG3B (*FP*_3B) for '21AF'.

## 4. Discussion

*Fragaria x ananassa* is an octoploid species, its breeding programs being of great importance due to consumption levels of its highly valued fruit. Its polyploid nature reduces the presence of major genes for trait variation and therefore, genetic heritability needs to be analysed as quantitative traits. Prior to QTL analysis, two SNP genetic maps were constructed from breeding lines. Four different parental lines, 'FC50', 'FD54', 'Camarosa' and 'Dover', with no family relationship, were chosen to develop the F1 ('FC50xFD54') and F2 ('21AF') populations. Despite the low number of seedlings at the end of analysis, the F1 population showed a high level of polymorphism and trait variation.

The constructed map 'FC50xFD54' presented a higher number of segregating markers (14595) compared to previously described genetic maps [5,7,30–33]. Moreover, 'FC50xFD54', '21AF' in addition to two other genetic maps [7,32], were grouped into the expected 28 LGs, thereby confirming the appropriate selection of parental lines. On average, the LGs of the 'FC50xFD54' genetic map represented more than 95 % of genome coverage. Only two LGs; LG1B and LG7C did not contain a good chromosome coverage, in addition to three gaps greater than 20 cM in LG1C, LG4B and LG7C, which indicates that these regions are not polymorphic in the two parental lines. Seven LGs of the '21AF' map covered less than 80 % of the genome and had large gaps. The low polymorphism in the F2 population was unexpected considering the
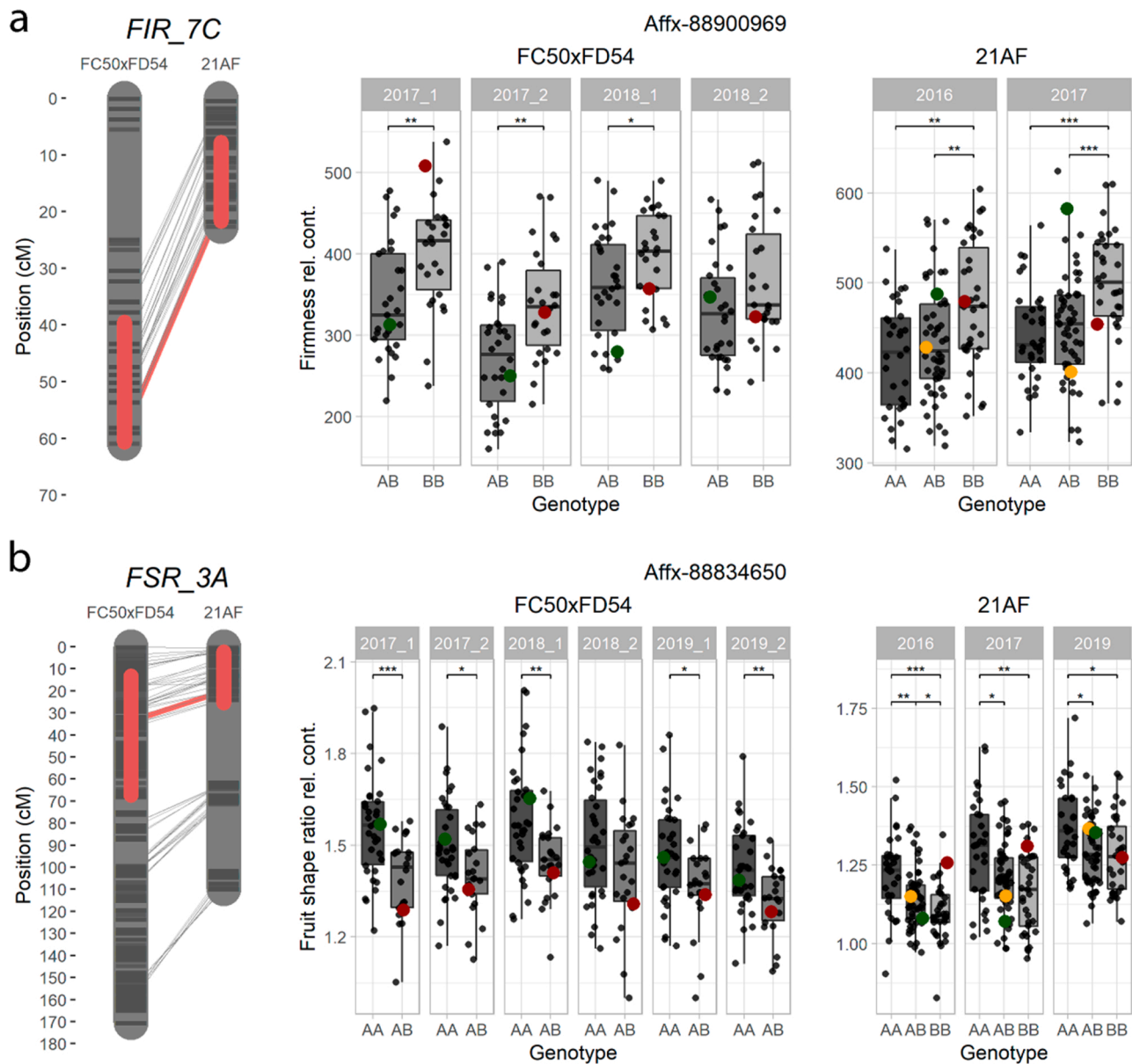
**Fig. 4. Shared QTLs of firmness and shape ratio.** a) *FIR_7C* and b) *FSR_3A*. Left: LG synteny representation showing marker position (grey), 1-LOD confidence interval (red boxes), marker synteny (grey lines) and the marker synteny used for the boxplot (red line). Right: boxplot for the selected marker in both populations in different harvests. Dots represent parental line (red), maternal line (green), siblings (black) and 'H-21' (yellow). Significant levels are <0.001 (***), <0.01 (**), <0.05 (*) and <0.1 (') (For interpretation of the references to colour in this figure legend, the reader is referred to the web version of this article.).

genetic distance between the parental lines. Indeed, only 9 % of the SNP markers from the IStraw90k array mapped in the '21AF' population, while the proportion is about 35 % when using the IStraw35k array for the 'FC50xFD54' population. Both arrays were constructed using the *F. vesca* genome and it is not easy to locate the position of the markers in the *F. x ananassa* genome [9]. However, there was good genome coverage and a high collinearity between genetic and physical positions in both populations (Fig. 1 and Supplementary Fig. 1), confirming that these genetic maps were well constructed. The four parental lines are distant and highly heterozygous, the low coverage seen in the '21AF' map could be due to the loss of heterozygosity in the hybrid 'H-21' used to develop the F2 population. As expected, the size of maps generated after discarding markers with unlikely genotypes or with many missing data was reduced. The F2 map was about 10 % shorter, but in the F1 map the size reduction was about one third, which we attribute to the fact that, given that this map was done with many more markers (almost twice), more markers with erroneous data were discarded, resulting in a

larger overall reduction of total distance due to inaccurate genotyping.

Strawberry fruit quality traits have been described as highly environmental-dependent and their corresponding QTLs were distributed along the whole genome [2–4]. However, a large number of stable QTLs (33) were mapped in the 'FC50xFD54' population and seven major QTLs (LOD > 4) were detected, explaining around 30 % of trait variation, while only eight stable QTLs were found in the '21AF' population. However, before comparing the number of stable QTLs in the two maps, it is important to note that phenotyping for both populations was carried out over a period of three years, data for the 'FC50xFD54' population was taken from two harvests per year, while the '21AF' population for only a single harvest per year. To consider a QTL stable, it must be found at least twice. Since six harvests were counted for 'FC50xFD54' versus three for '21AF', it was easier to find stable QTLs for the first population than for the second. To evaluate the possible differences between early and late season for the different traits, two harvests per year were analysed in 'FC50xFD54', but no significant differences were found,

indicating the independence of the two events. Given that we analysed several harvests, the differences in stability found in these QTLs could be explained by the mode of action of each QTL, one being the most important and stable, the others modulating the trait based on environmental conditions.

Previous QTL analyses of fruit quality traits have used genetic maps with marker densities lower than those in our maps [2–4] finding also several QTLs in different homeologous groups (HGs). Since SSRs and AFLP markers are not sub-genome determined, it is quite difficult to compare HGs between maps. Comparisons with previous studies are quite challenging, especially when QTLs for the same trait are mapped to different homeologous groups, such as fruit shape traits in LG4C and LG4D or LG6A and LG6C as detected in our map.

For fruit quality traits, the present QTL analysis revealed that they were located across the genome. In our populations, two fruit weight QTLs, *FW_1A* and *FW_*3A explaining 27 and 23 % of trait variability respectively, were detected, which could be related to those previously described by Zorrilla-Fontanesi et al., in 2011 and Lerceteau-Köhler et al., in 2012. In addition, the fruit weight correlated with two other shape traits, the length and diameter of the fruit, with each one explaining more than 20 % of the trait variation. These correlations have been mentioned previously [3].

Regarding taste traits, several QTLs have been mapped across the genome [2–4]. *TA_5A* and *pH_5D* QTLs detected in this study are in agreement with the acidity and organic acids QTLs previously mapped in a different HG5 [2,12], and a new major and shared QTL was found for TA and SAR in LG1A (34 % of variation). Although several SSC QTLs of minor significance have been described [2–4], no genomic region has been found that explains the variance presented in our SSC analysis. This indicates the complexity and instability of the SSC trait, which in part involve rapid chemical changes in harvested fruits related to the conditions of handling and storage, prior to SSC analysis, and which cannot be controlled.

One of the most important traits for postharvest handling and transport is related to quality and firmness of fruit, a complex character linked to ripening and which involves several coordinated cell-wall degrading enzymes. Despite its complexity, a strong *FIR_7C* QTL was identified in both 'FC50xFD54' and '21AF' populations as previously reported in LGVII-1 [2]. Since this QTL was found in both populations (Table 2, Fig. 4a), a relatively short genomic region of 1.5 Mb was delimited and a representative marker was identified that could be used in marker assisted selection (MAS) (Fig. 4a) to improve firmness in strawberry breeding programs. Two annotated genes in the region, expansin 2 and polygalacturonase, are known to be involved in cell-wall degradation, and hence associated with fruit firmness [34,35]. In the '21AF' population, another firmness QTL was mapped in LG1A, previously described in the same population, and postulated *FaRGlyase1* as a candidate gene [14].

The shape of strawberries can vary depending on many factors, such as environmental conditions, pollination and hormonal regulation, for instance auxins that are involved in the diameter of the fruits and gibberellic acids (GA) in the length [19]. In our populations, the fruit shape QTLs were distributed throughout the genetic map, but three hotspots were distinguished in LG3A, LG4D and LG6C. The *FSR_3A* QTL was mapped in both populations and it could be related to either of the two homeologous QTLs described previously [3]. Additionally, new QTLs in HG4 were discovered, such as *FSR_4C* for circular shape and *FSR_4D* for ovoid shape. The *FD_2A* QTL is also in agreement with the round QTL detected in LG2 in a diploid NILs collection [11].

A segregating neck phenotype, an undesirable trait for breeding, was observed in the 'FC50xFD54' population, and two QTLs were mapped, the first, *Neck_3A*, a major and stable QTL explaining 35.5 % of the variance of the trait; and the second, *Neck_4A*, which is also a major QTL. Since visual phenotyping of this trait can be time-consuming and complicated, it was suggested that the WWP trait, an objective measure for more accurate mapping of QTLs, be used instead. The SNPs linked to the measured WWP ratio could be useful in breeding programs for discarding undesirable neck phenotypes.

The quality and appearance traits of the fruit are polygenic and, to enhance these traits, several associated markers need to be improved. Validation of the markers in different populations means they could be used for marker assisted selection in different genetic backgrounds.

## 5. Conclusions

The genetic characterization of fruit quality traits in cultivated strawberry using genetic maps of two non-related F1 and F2 populations, showed high collinearity and synteny between the maps and between both maps and the genome. Our in-depth characterization of fruit traits such as taste, firmness and shape in two different populations, from different harvests, in different locations over a period of three years, gave 41 QTLs, thereby clarifying the subgenome localization of previously reported QTLs, including the regions responsible for juice acidity, flavour index, and shape ratio for more elongated fruits and firmness. Two markers should be highlighted, one linked to the variation in fruit firmness in linkage group *FIR_7C*, and another to the variation in the shape ratio in *FSR_3A*. These QTLs were consistent in the two studied populations, both of which had different genetic backgrounds, suggesting therefore that these markers are in fact appropriate for use in MAS for strawberry breeding programs.

## Declaration of Competing Interest

The authors declare that they have no known competing financial interests or personal relationships that could have appeared to influence the work reported in this paper.

## Appendix A. Supplementary data

Supplementary material related to this article can be found, in the online version, at doi:https://doi.org/10.1016/j.plantsci.2021.111010.

## References

[1] D.J. Sargent, J. Clarke, D.W. Simpson, K.R. Tobutt, P. Arús, A. Monfort, S. Vilanova, B. Denoyes-Rothan, M. Rousseau, K.M. Folta, N.V. Bassil, N.H. Battey, An enhanced microsatellite map of diploid *Fragaria*, Theor. Appl. Genet. 112 (2006) 1349–1359.

[2] Y. Zorrilla-Fontanesi, A. Cabeza, P. Domínguez, J.J. Medina, V. Valpuesta, B. Denoyes-Rothan, J.F. Sánchez-Sevilla, I. Amaya, Quantitative trait loci and underlying candidate genes controlling agronomical and fruit quality traits in octoploid strawberry (Fragaria x ananassa), Theor. Appl. Genet. 123 (2011) 755–778, https://doi.org/10.1007/s00122-011-1624-6.

[3] E. Lerceteau–Köhler, A. Moing, G. Guérin, C. Renaud, A. Petit, C. Rothan, B. Denoyes, Genetic dissection of fruit quality traits in the octoploid cultivated strawberry highlights the role of homoeo-QTL in their control, Theor. Appl. Genet. 124 (2012) 1059–1077, https://doi.org/10.1007/s00122-011-1769-3.

[4] P. Castro, K.S. Lewers, Identification of quantitative trait loci (QTL) for fruit-quality traits and number of weeks of flowering in the cultivated strawberry, Mol. Breed. 36 (2016), https://doi.org/10.1007/s11032-016-0559-7.

[5] N.V. Bassil, T.M. Davis, H. Zhang, S. Ficklin, M. Mittmann, T. Webster, L. Mahoney, D. Wood, E.S. Alperin, U.R. Rosyara, H. Koehorst-vanc Putten, A. Monfort, D. J. Sargent, I. Amaya, B. Denoyes, L. Bianco, T. van Dijk, A. Pirani, A. Iezzoni, D. Main, C. Peace, Y. Yang, V. Whitaker, S. Verma, L. Bellon, F. Brew, R. Herrera, E. van de Weg, Development and preliminary evaluation of a 90 K Axiom® SNP

array for the allo-octoploid cultivated strawberry Fragaria × ananassa, BMC Genomics 16 (2015) 155–185, https://doi.org/10.1186/s12864-015-1310-1.

[6] S. Verma, N.V. Bassil, E. van de Weg, R.J. Harrison, A. Monfort, J.M. Hidalgo, I. Amaya, B. Denoyes, L. Mahoney, T.M. Davis, Z. Fan, S. Knapp, V.M. Whitaker, Development and evaluation of the Axiom® IStraw35 384HT array for the allo-octoploid cultivated strawberry Fragaria × ananassa, Acta Hortic. (2017) 75–82, https://doi.org/10.17660/ActaHortic.2017.1156.10.

[7] H.M. Cockerton, R.J. Vickerstaff, A. Karlstrom, F. Wilson, M. Sobczyk, J.Q. He, D. J. Sargent, A.J. Passey, K.J. McLeary, K. Pakozdi, N. Harrison, M. Lumbreras-Martinez, L. Antanaviciute, D.W. Simpson, R.J. Harrison, Identification of powdery mildew resistance QTL in strawberry (Fragaria x ananassa), Theor. Appl. Genet. 131 (2018) 1995–2007, https://doi.org/10.1007/s00122-018-3128-0.

[8] H.M. Cockerton, B. Li, R.J. Vickerstaff, C.A. Eyre, D.J. Sargent, A.D. Armitage, C. Marina-Montes, A. Garcia-Cruz, A.J. Passey, D.W. Simpson, R.J. Harrison, Identifying verticillium dahliae resistance in strawberry through disease screening of multiple populations and image based phenotyping, Front. Plant Sci. 10 (2019) 924, https://doi.org/10.3389/fpls.2019.00924.

[9] P.P. Edger, T.J. Poorten, R. VanBuren, M.A. Hardigan, M. Colle, M.R. McKain, R. D. Smith, S.J. Teresi, A.D.L. Nelson, C.M. Wai, E.I. Alger, K.A. Bird, A.E. Yocca, N. Pumplin, S. Ou, G. Ben-Zvi, A. Brodt, K. Baruch, T. Swale, L. Shiue, C. B. Acharya, G.S. Cole, J.P. Mower, K.L. Childs, N. Jiang, E. Lyons, M. Freeling, J. R. Puzey, S.J. Knapp, Origin and evolution of the octoploid strawberry genome, Nat. Genet. 51 (2019) 541–547, https://doi.org/10.1038/s41588-019-0356-4.

[10] M.A. Hardigan, M.J. Feldmann, A. Lorant, K.A. Bird, R. Famula, C. Acharya, G. Cole, P.P. Edger, S.J. Knapp, Genome synteny has been conserved among the octoploid progenitors of cultivated strawberry over millions of years of evolution, Front. Plant Sci. 10 (2020) 1789, https://doi.org/10.3389/fpls.2019.01789.

[11] M. Urrutia, J. Bonet, P. Arús, A. Monfort, A near-isogenic line (NIL) collection in diploid strawberry and its use in the genetic analysis of morphologic, phenotypic and nutritional characters, Theor. Appl. Genet. 128 (2015) 1261–1275, https://doi.org/10.1007/s00122-015-2503-3.

[12] J.G. Vallarino, D.M. Pott, E. Cruz-Rus, L. Miranda, J.J. Medina-Minguez, V. Valpuesta, A.R. Fernie, J.F. Sanchez-Sevilla, S. Osorio, I. Amaya, Identification of quantitative trait loci and candidate genes for primary metabolite content in strawberry fruit, Hortic. Res. 6 (2019) 4, https://doi.org/10.1038/s41438-018-0077-3.

[13] M. Draye, P. Van Cutsem, Pectin methylesterases induce an abrupt increase of acidic pectin during strawberry fruit ripening, J. Plant Physiol. 165 (2008) 1152–1160, https://doi.org/10.1016/j.jplph.2007.10.006.

[14] F.J. Molina-Hidalgo, A.R. Franco, C. Villatoro, L. Medina-Puche, J.A. Mercado, M. A. Hidalgo, A. Monfort, J.L. Caballero, J. Munoz-Blanco, R. Blanco-Portales, The strawberry *(Fragaria x ananassa)* fruit-specific *rhamnogalacturonate lyase 1* (*FaRGLyase1*) gene encodes an enzyme involved in the degradation of cell-wall middle lamellae, J. Exp. Bot. 64 (2013) 1471–1483, https://doi.org/10.1093/jxb/ers386.

[15] S. Pose, A.R. Kirby, C. Paniagua, K.W. Waldron, V.J. Morris, M.A. Quesada, J. A. Mercado, The nanostructural characterization of strawberry pectins in pectate lyase or polygalacturonase silenced fruits elucidates their role in softening, Carbohydr. Polym. 132 (2015) 134–145, https://doi.org/10.1016/j.carbpol.2015.06.018.

[16] C. Paniagua, N. Santiago-Domenech, A.R. Kirby, A.P. Gunning, V.J. Morris, M. A. Quesada, A.J. Matas, J.A. Mercado, Structural changes in cell wall pectins during strawberry fruit development, Plant Physiol. Biochem. 118 (2017) 55–63, https://doi.org/10.1016/j.plaphy.2017.06.001.

[17] A. Mendez-Yanez, M. Gonzalez, C. Carrasco-Orellana, R. Herrera, M.A. Moya-Leon, Isolation of a rhamnogalacturonan lyase expressed during ripening of the Chilean strawberry fruit and its biochemical characterization, Plant Physiol. Biochem. 146 (2020) 411–419, https://doi.org/10.1016/j.plaphy.2019.11.041.

[18] G.M. Symons, Y.-J. Chua, J.J. Ross, L.J. Quittenden, N.W. Davies, J.B. Reid, Hormonal changes during non-climacteric ripening in strawberry, J. Exp. Bot. 63 (2012) 4741–4750, https://doi.org/10.1093/jxb/ers147.

[19] L. Liao, M. Li, B. Liu, M. Yan, X. Yu, H. Zi, H. Liu, C. Yamamuro, Interlinked regulatory loops of ABA catabolism and biosynthesis coordinate fruit growth and ripening in woodland strawberry, Proc. Natl. Acad. Sci. 49 (2018) 11542–11550, https://doi.org/10.1073/pnas.1812575115.

[20] J.J. Doyle, J.L. Doyle, Isolation of plant DNA from fresh tissue, Focus 12 (1990) 13–15.

[21] J.W. van Ooijen, JoinMap ® 5, Software for the Calculation of Genetic Linkage Maps in Experimental Population of Diploid Species, Kyazma B.V., Wageningen, Netherlands, 2018.

[22] D.D. Kosambi, The estimation of map distances from recombination values, Ann. Eugen. 12 (1944) 172–175, https://doi.org/10.1111/j.1469-1809.1943.tb02321.x.

[23] M.A. Hardigan, A. Lorant, D.D.A. Pincot, M.J. Feldmann, R.A. Famula, C. B. Acharya, S. Lee, S. Verma, V.M. Whitaker, N. Bassil, J. Zurn, G.S. Cole, K. Bird, P. P. Edger, S.J. Knapp, Unraveling the complex hybrid ancestry and domestication history of cultivated strawberry, Mol. Biol. Evol. (2021), https://doi.org/10.1093/molbev/msab024.

[24] P.P. Edger, R. VanBuren, M. Colle, T.J. Poorten, C.M. Wai, C.E. Niederhuth, E. I. Alger, S. Ou, C.B. Acharya, J. Wang, P. Callow, M.R. McKain, J. Shi, C. Collier, Z. Xiong, J.P. Mower, J.P. Slovin, T. Hytonen, N. Jiang, K.L. Childs, S.J. Knapp, Single-molecule sequencing and optical mapping yields an improved genome of woodland strawberry (Fragaria vesca) with chromosome-scale contiguity, GigaScience 7 (2018) 1–7, https://doi.org/10.1093/gigascience/gix124.

[25] A. Darrigues, J. Hall, E. van der Knaap, D.M. Francis, N. Dujmovic, S. Gray, Tomato Analyzer-color test: a new tool for efficient digital phenotyping, J. Am. Soc. Hortic. Sci. 133 (2008) 579–586.

[26] M.J. Gonzalo, M.T. Brewer, C. Anderson, D. Sullivan, S. Gray, E. van der Knaap, Tomato fruit shape analysis using morphometric and morphology attributes Implemented in Tomato Analyzer software program, J. Am. Soc. Hortic. Sci. 134 (2009) 77–87.

[27] RCoreTeam, R: a Language and Environment for Statistical Computing, R Foundation for Statistical Computing, Vienna, Austria, 2019.

[28] RStudio, RStudio: Integrated Development Environment for R Version 0.98.1049 Ed, RStudio, Boston, MA, USA, 2019.

[29] J. van Ooijen, MapQTL 6. Software for the Mapping of Quantitative Trait Loci in Experimental Populations of Diploid Species, Kyazma BV, Wageningen, Netherlands, 2009.

[30] D.J. Sargent, Y. Yang, N. Surbanovski, L. Bianco, M. Buti, R. Velasco, L. Giongo, T. M. Davis, HaploSNP affinities and linkage map positions illuminate subgenome composition in the octoploid, cultivated strawberry (Fragariaxananassa), Plant Sci. 242 (2016) 140–150, https://doi.org/10.1016/j.plantsci.2015.07.004.

[31] S. Nagano, K. Shirasawa, H. Hirakawa, F. Maeda, M. Ishikawa, S.N. Isobe, Discrimination of candidate subgenome-specific loci by linkage map construction with an S1 population of octoploid strawberry (Fragaria x ananassa), BMC Genomics 18 (2017) 374, https://doi.org/10.1186/s12864-017-3762-y.

[32] A. Anciro, J. Mangandi, S. Verma, N. Peres, V.M. Whitaker, S. Lee, FaRCg1: a quantitative trait locus conferring resistance to Colletotrichum crown rot caused by Colletotrichum gloeosporioides in octoploid strawberry, Theor. Appl. Genet. 131 (2018) 2167–2177, https://doi.org/10.1007/s00122-018-3145-z.

[33] D.J. Sargent, M. Buti, N. Surbanovski, M.B. Brurberg, M. Alsheikh, M.P. Kent, J. Davik, Identification of QTLs for powdery mildew (Podosphaera aphanis; syn. Sphaerotheca macularis f. sp. fragariae) susceptibility in cultivated strawberry (Fragaria xananassa), PLoS One 14 (2019), e0222829, https://doi.org/10.1371/journal.pone.0222829.

[34] C.F. Nardi, N.M. Villarreal, M.C. Dotto, M.T. Ariza, J.G. Vallarino, G.A. Martínez, V. Valpuesta, P.M. Civello, Influence of plant growth regulators on Expansin2 expression in strawberry fruit. Cloning and functional analysis of FaEXP2 promoter region, Postharvest Biol. Technol. 114 (2016) 17–28, https://doi.org/10.1016/j.postharvbio.2015.11.008.

[35] C. Paniagua, P. Ric-Varas, J.A. Garcia-Gago, G. Lopez-Casado, R. Blanco-Portales, J. Munoz-Blanco, J. Schuckel, J.P. Knox, A.J. Matas, M.A. Quesada, S. Pose, J. A. Mercado, Elucidating the role of polygalacturonase genes in strawberry fruit softening, J. Exp. Bot. 71 (2020) 7103–7117, https://doi.org/10.1093/jxb/eraa398.